**Steel and Composite Structures**, *Vol. 30, No. 5 (2019) 417-432*
DOI: https://doi.org/10.12989/scs.2019.30.5.417


# Behavior study of NC and HSC RCCs confined by GRP casing and CFRP wrapping

Fathollah Sajedi *1 and Mahdi Shariati **2

[1] *Department of Civil Engineering, Ahvaz Branch, Islamic Azad University, Ahvaz, Iran*
[2] *Faculty of Civil Engineering, University of Tabriz, Tabriz, Iran*

(*Received November 4, 2018, Revised December 21, 2018, Accepted March 1, 2019*)

**Abstract.** This paper presents the results of axial compression testing and numerical modeling on reinforced concrete columns (RCC) with normal concrete (NC) and high-strength concrete (HSC), RCC confined by glass-fiber reinforced plastic pipes (GRP) casing as well as carbon fiber reinforced polymer (CFRP), The major parameters evaluated in the experiments were the effects of concrete type, GRP casing and CFRP wrapping, as well as the number of CFRP layers. 12 cylindrical RCC (150×600 mm) were prepared and divided into two groups, NC and HSC. Each group was divided into two parts; with and without GRP casing. In each part, one column was without CFRP strengthening layer, a column was wrapped with one CFRP layer and another column with two CFRP layers. All columns were tested under concentrated compression load. Numerical modeling was performed using ABAQUS software and the results of which were compared with experimental findings. A good agreement was found between the results. Results indicated that the utilization of CFRP wrapping and GRP casing improved compression capacity and ductility of RCC. The addition of one and two layer-FRP wrapping increased capacity in the NC group to an average of 18.5% and 26.5% and in the HSC group to an average of 10.2% and 24.8%. Meanwhile, the utilization of GRP casing increased the capacity of the columns by 3 times in the NC group and 2.38 times in the HSC group. The results indicated that although both CFRP wrapping and GRP casing increased confinement, the GRP casing gave more increase capacity and ductility of the RCC due to higher confinement. Furthermore, the confinement effect was higher on NC group.

**Keywords:** Reinforced Concrete Columns (RCC); GRP casing; CFRP wrapping; High Strength Concrete (HSC); axial force; ductility; numerical modeling

## 1. Introduction

There are various reasons for retrofitting concrete structures; aging, erosion under environmental conditions, changes in usage, increased loadings, development of existing structures, earthquake damage, and other natural disasters, and non-compliance with the new design code are reasons for retrofitting reinforced concrete structures (RCC) (Hamidian *et al*. 2011, 2012, Shariati 2008, Shariati *et al*. 2011a, b, c, Sinaei *et al*. 2011). One of the common methods of retrofitting and increasing the load capacity of RCC is confining them by FRP material (Abedini *et al*. 2017, Sharbatdar *et al*. 2008, Sinaei *et al*. 2011). The confinement of reinforced concrete columns restricts their radial expansion followed by a delay in concrete shell detachment which prevents the buckling of longitudinal bars in the column, thereby delaying column failure, eventually (Tokgoz *et al*. 2012).

HSC is considered a rather novel material and has been developed over the last years (Hamidian *et al*. 2011, Khorramian *et al*. 2015, Mohammadhassani *et al*. 2014a, b, Shariati 2014, Shariati *et al*. 2011a, b, c, 2012, 2014a, b, 2015, 2016). The advantages of these concrete include high compression and tension strengths, higher modulus of elasticity and lower porosity (Le *et al*. 2017). Nevertheless, RCC made of HSC exhibit more brittle behavior than NC concrete columns; therefore, these columns require strengthening in order to enhance ductility (Shariati *et al*. 2011a, b, c). Strengthening RCC by wrapping them with CFRP is a method that has recently been utilized. The CFRP layers can be easily installed on the surface of concrete columns, and in terms of economic and implementation speed; it is a very appropriate option (Abedini *et al*. 2017, Andalib *et al*. 2018, Bazzaz *et al*. 2018, Dundar *et al*. 2015, Goodarzi *et al*. 2009, Kazemi *et al*. 2012, Momenzadeh *et al*. 2017, Paknahad *et al*. 2018).

Until now, lots of researches have been conducted on the behavior of reinforced cylindrical concrete columns with CFRP wrapping. (Khairallah 2013, Shahawy *et al*. 2000, Sheikh 2002, Wong *et al*. 2008) investigated RCC with circular section using CFRP wrapping and concluded that the use of FRP materials increased the compressive capacity and ductility of confined concrete columns by affecting the concrete core under compressive loads. (Kumutha *et al*. 2007, Parvin and Jamwal 2005, Rahai *et al*. 2008) investigated the effect of number of FRP strengthening layers applied on the surface of concrete columns and concluded that utilizing more layers and

∗Corresponding author, Ph.D., Professor,
E-mail: sajedi@iauahvaz.ac.ir; f_sajedi@yahoo.com

∗∗Co-corresponding author, Ph.D.,
E-mail: shariati@tabriz.ac.ir


http://www.techno-press.org/?journal=scs&subpage=6 ISSN: 1229-9367 (Print), 1598-6233 (Online)

thicker sheets would increase the compression capacity of reinforced columns. Besides, fiber and fiber tissue type, the amount of resin and other factors affect strengthening percentage. (Almusallam 2007, Vincent and Ozbakkaloglu 2013) examined the strengthening percentage created with FRP sheets for columns made of NC and HSC. They concluded that the amount of strengthening created was lower in HSC columns with the probable reason being the lower strength created by the confinement layer relative to the compression strength of the concrete (Mohammadhassani *et al*. 2015, Sadeghipour Chahnasir *et al*. 2018, Toghroli *et al*. 2018a, b).

Recently, studies have been performed on composite columns, which are concrete columns filled with GRP pipes. In these columns, GRP pipes act as a durable framework and provide radial confinement for column core and limit the rupture of micro-cracks. At the same time, the concrete core prevents the buckling of GRP casing. (Xiao *et al*. 2014) investigated both reinforced and unreinforced concrete columns confined in GRP casings. The results of these studies showed that GRP casing increased compression strength, hardness, and ductility of confined columns in the GRP casing. Tested under eccentric loading, it was reported that GRP confined column performance was better than columns without casing. (Khanouki *et al*. 2016, Pessiki *et al*. 2001) investigated cylindrical concrete columns with GRP casing inner core and showed that the columns had higher compression capacity and better ductility than columns without casing (Aghaee and Foroughi 2013, Ardalan *et al*. 2017, Joshaghani 2017, Khorami *et al*. 2017).

The purpose of this research is an experimental and numerical study of the individual and simultaneous effects of GRP casing and CFRP wrapping on RCC made with NC and HSC with circular section which was obtained by constructing 12 reinforced concrete cylinder specimens of 150 mm diameter and 600 mm height, and compressive strength tests and determination of their axial and radial deformation were conducted. Besides, 3D modeling and numerical analysis were performed using ABAQUS finite element software (ABAQUS 2011). The results of finite element model analysis were compared with experimental results.

## 2. Behavior of confined concrete columns

The core of concrete columns subjected to axial loading expands radially based on the Poisson effect. FRP confinement prevents this expansion and triaxial compression on concrete increases its axial strength. Eq. (1) has been proposed by Csuka and Kolla´r in order to determine the FRP lateral confining stress to the cylindrical concrete columns (Csuka and Kollár 2010); where, $\sigma_l$, $\sigma_f$, $t$ and $d$ represent the lateral confining stress, FRP tensile stress, FRP thickness, and diameter of the cylindrical column, respectively.

$$\sigma_l = \frac{2\sigma_f t}{d} \tag{1}$$

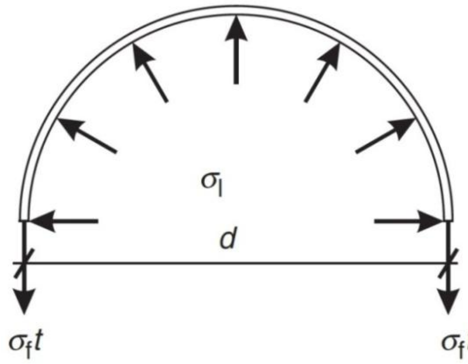


Fig. 1 The confining stress of the FRP wrapping on the surface of the cylindrical concrete column (Csuka and Kollár 2010)

The FRP tensile stress is calculated from Eq. (2), where, $E_f$ is the elastic modulus of the FRP wrapping and $\mathcal{E}_f$ denotes the FRP radial strain.

$$\sigma_f = E_f \varepsilon_f \tag{2}$$

The confining stress of the FRP wrapping is demonstrated in Fig. 1.

### 2.1 Stress-strain curve of confined concrete

The stress-strain curve of the unconfined concrete column, as displayed in Fig. 2(a), is decreasing after reaching the pick compressive stress. On the other hand, the stress-strain curve of the concrete column confined with the FRP wrapping depends on the adequacy or inadequacy of the confinement created by the FRP wrapping. In the case of sufficient confinement, the stress-strain curve is either steadily increasing, as shown in Fig. 2(b) and is approximately bi-linear, or is descending after reaching the pick stress as revealed in Fig. 2(c). In case of insufficient confinement, the stress-strain curve is also decreasing after reaching the pick compressive stress, as demonstrated in Fig. 2(d). In this case, the ultimate compressive strength will be less than the maximum compressive strength of the unconfined concrete column (Csuka and Kollár 2010).

In Fig. 2, the parameters $f_{c0}$, $f_{cc}$ *and* $f_{cu}$ represent the compressive strength of concrete, compressive strength of the confined concrete, and compressive stress in confined concrete at rupture of confinement, respectively.

So far, different equations have been proposed to predict the compressive strength of the confined concrete with FRP ($f_{cc}$), These are equations provided by (Lam and Teng 2003, Saafi *et al*. 1999, Samaan *et al*. 1998, Wu *et al*. 2006, Xiao and Wu 2000, Youssef *et al*. 2007)as presented in Table 1.

## 3. Mechanical properties of CFRP wrapping and GRP casing

The used composite layers in this research are uniaxial CFRP made by TORAY Co. The mechanical properties of

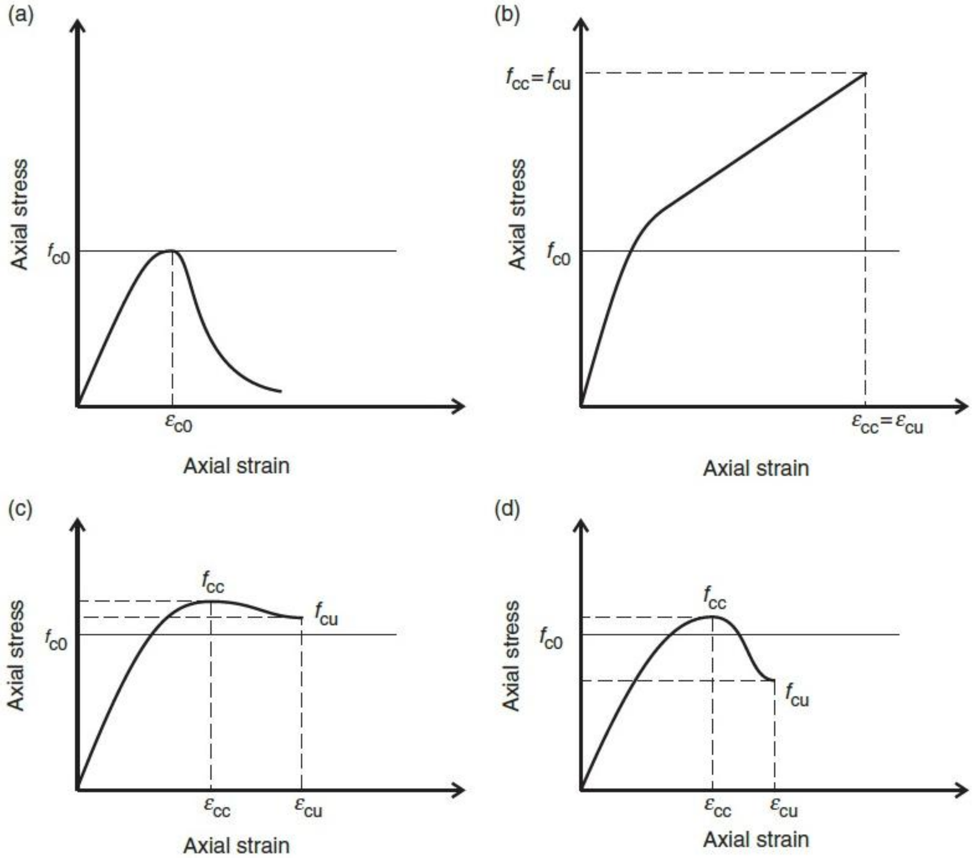


Fig. 2 Stress-strain curve of (a) unconfined concrete column; (b) Column with sufficient confinement with monotonic curve; (c) Column with sufficient confinement with diminishing second part; (d) column with insufficient confinement

CFRP material were provided based on the manufacturing company's information and the tests based on ASTM D7565 (Testing and Materials 2004) standard are presented in Table 2. The used epoxy resin was made by Paya Co. in two-partials of resin and stiffener. The tolerable tensile stress of resin is 30 MPa and the tensile rupture strain is 3.6%. The characteristic of the mentioned resin was obtained based on the reports of the manufacturing company and the conducted tests were based on ASTM D638 standard (Plastics 2010).

GRP composite casings are made in Mashhad Sadra Shargh factory and their mechanical properties are based on the manufacturer's data based on ASTM D2996 standard (ASTM 2001) are presented in Table 2.

Table 1 Equations for prediction of compressive strength of the confined concrete

| Reference | Equation |
|---|---|
| (Samaan *et al.* 1998) | $\frac{f_{cc}}{f_{c0}} = 1 + 6.0\frac{f_l^{0.7}}{f_{c0}}$ |
| (Saafi *et al.* 1999) | $\frac{f_{cc}}{f_{c0}} = 1 + 2.2\left(\frac{f_l}{f_{c0}}\right)^{0.84}$ |
| (Lam and Teng 2003) | $\frac{f_{cc}}{f_{c0}} = 1 + 2\frac{f_l}{f_{c0}}$ |
| (Youssef *et al.* 2007) | $\frac{f_{cc}}{f_{c0}} = 1 + 2.25\left(\frac{f_l}{f_{c0}}\right)^{1.25}$ |
| (Wu *et al.* 2006) | $\frac{f_{cc}}{f_{c0}} = 0.745 + 3.357\frac{f_l}{f_{c0}} - 1.053\left(\frac{f_l}{f_{c0}}\right)^2$ |
| (Xiao and Wu 2000) | $\frac{f_{cc}}{f_{c0}} = 1.1 + \left[4.1 - 0.75\left(\frac{f_{c0}^2}{E_l}\right)\right]\frac{f_l}{f_{c0}}$ where $E_l = \frac{2E_f t}{d}$ |

Table 2 The mechanical properties of CFRP material and GRP composite casings (ASTM 2001, Testing and Materials 2004)

| Composite characteristics | CFRP material | GRP casing |
|---|---|---|
| Thickness (mm) | 0.166 | 8 |
| Density (kg/m$^3$) | 1900 | 1800 |
| Weight in surface unit (g/m$^2$) | 300 | - |
| Weight in length unit (g/m) | - | 6786 |
| Tensile stress (MPa) | 4900 | 75 |
| Modulus of elasticity (GPa) | 230 | 120 |
| Poisson ratio | 0.3 | 0.4 |
| Final strain (%) | 2.5 | 1.3 |

## 4. Experimental program

### *4.1 Preliminary tests*

NC and HSC were used to construct the columns of this study; the details of mixing design for 1 $m^3$ of the consumed concrete are presented in Table 3.

In order to determine compressive strength of concretes used for columns construction, cylindrical specimens with 150 mm diameter and 300 mm height were prepared according to recommendation of ACI-211 (211, 1991) and after 28 days curing in water pond, their mean compressive strength were 32.7 MPa and 63.1 MPa for NC and HSC, respectively.

### *4.2 Specimens' characteristics*

The experimental specimens of this research included 12 concrete columns with circular section having 150 mm diameter and 600 mm height. Columns were prepared and divided into two group, NC and HSC, and each group was divided into two part; with and without GRP casing. In each part, one column was without FRP layer, a column was wrapped with one FRP layer and another column with two FRP layers. All columns were reinforced concrete.

Table 3 Concrete mixing design

| Mix constituents | NC (kg/$m^{3)}$ | HSC (kg/$m^{3)}$ |
|---|---|---|
| Cement type 2 | 350 | 550 |
| Water | 157.5 | 111.5 |
| Gravel | 932 | 930 |
| Sand | 932 | 720 |
| Micro-silica gel | - | 55 |
| SP | - | 2.5 |
| w/c | 0.45 | 0.45 |

Table 4 Characteristics of the laboratory specimens of research

| Specimen name | GRP casing | CFRP wrapping | CFRP Layer no. |
|---|---|---|---|
| N | NO | NO | 0 |
| NF1 | NO | YES | 1 |
| NF2 | NO | YES | 2 |
| GN | YES | NO | 0 |
| GNF1 | YES | YES | 1 |
| GNF2 | YES | YES | 2 |
| H | NO | NO | 0 |
| HF1 | NO | YES | 1 |
| HF2 | NO | YES | 2 |
| GH | YES | NO | 0 |
| GHF1 | YES | YES | 1 |
| GHF2 | YES | YES | 2 |

Columns were named according to their components as follows: For column with HSC H, column with NC N, column with CFRP wrapping F and column with GRP casing G was considered. Number after F shows the number of CFRP layers in columns having CFRP wrapping. Table 4 presents characteristics of columns.

### *4.3 Preparing specimens*

The experimental specimens of this research included 12 concrete columns and 2 specimens were considered to be used as storage in the experiments. The used longitudinal reinforcement was considered as 2.7% of the gross cross-section of the column in all columns which were supplied using 6 ribbed bars with a diameter of 10 mm. The longitudinal bars were cut at a distance of 20 mm at both ends of the columns to prevent stress concentration on them. Thus, the considered length of the longitudinal bars was 560 mm. Moreover, spiral bars with 80 mm pitch and 6 mm diameter were used on each network. The concrete coverage on the bars was considered as 25 mm. Spacer was used to provide the mentioned coverage for the longitudinal and spiral bars. The tensile stresses of longitudinal and transverse reinforcements were 400 MPa and 300 MPa respectively, based on the manufacturer's data. Fig. 3 presents the longitudinal and cross sections of the studied columns. To measure the strain of bars during columns compressive testing, digital strain-gage was used to examine the columns' behavior. Therefore, the strain-gages were installed on the bars before casting of each column. Fig. 4(a) presents the installment of this strain-gage. Oil was sprayed on the internal surface of the framework for easy separation from concrete surface and reinforcement was put in the framework.

Fig. 4(b) presents the reinforcement placement inside GRP casing. NC and HSC were used for casting and the slumps were 80 mm and 210 mm, respectively. For curing, columns were put in water pond for 28 days. To prepare the

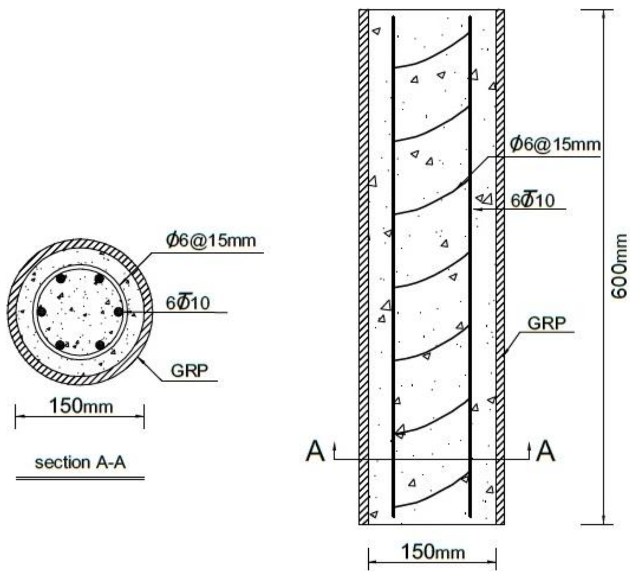


Fig. 3 Longitudinal and Cross section of research columns

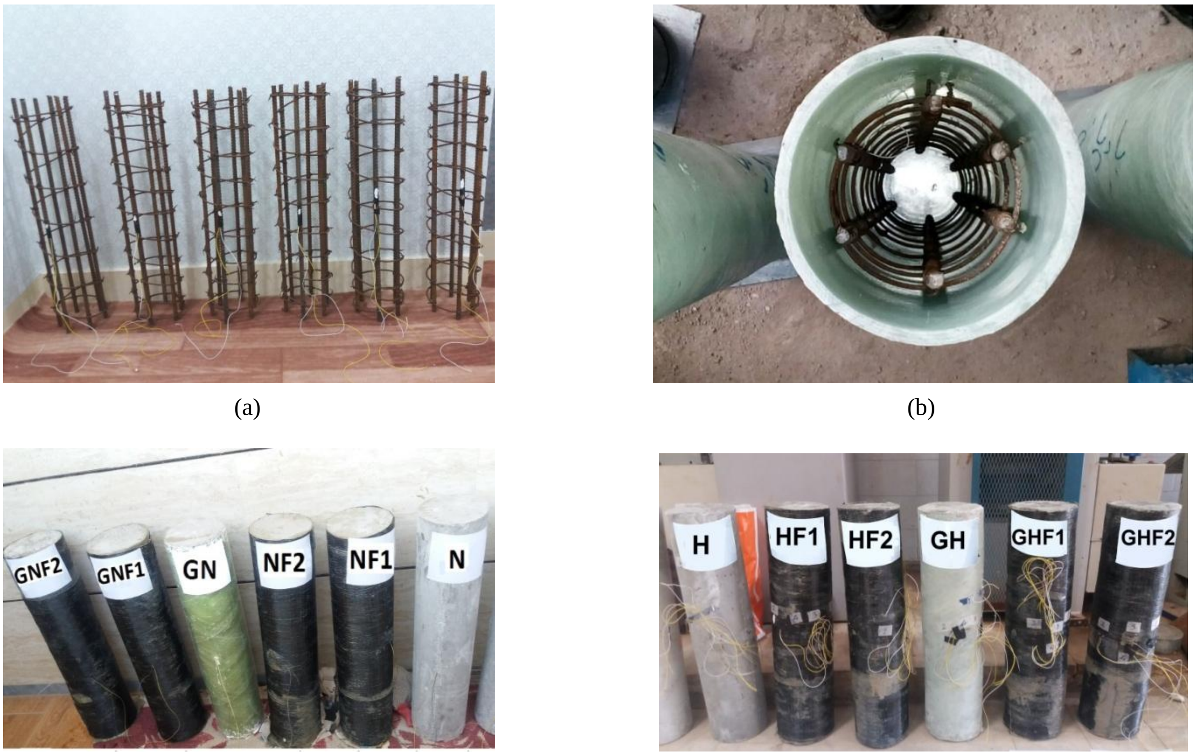


(a) (b) (c) (d)

Fig. 4 Column preparing: (a) Strain-gage installation on bars; (b) Placement reinforcement inside GRP casings; (c) NC group; (d) HSC group

concrete columns for installation of the CFRP layers before applying epoxy resin, first the external surface of columns were completely smoothened, cleaned, and dried. The used epoxy resin was 2 partial and made of resin and hardener which were mixed manually in a ratio of 1:3 for 5 min, then the thin layer of resin was rubbed on the concrete cylindrical surface and CFRP layer was carefully wrapped around the column. The end edge of CFRP wrapping was overlapped at 100 mm to ensure non-separation. The second layer was wrapped 2 hours after installation of the first layer for columns with 2 CFRP layers. All columns were wrapped with zero angles and were kept in the room temperature for 7 days for curing of the epoxy resin. Figs. 4(c) and (d) presents the studied columns after installing CFRP wrap.

### *4.4 Testing the columns*

The columns of this research were tested under uniaxial pressure loading by hydraulic jack with 5000 kN capacity in the soil mechanic laboratory of the Road and Transportation office of Khuzestan province. Specimens were tested by displacement control method and a loading rate of 10 kN/s (Kent and Park 1971). Two axial strain-gage and one lateral strain-gage were installed in the middle of each column to determine the axial and lateral strains which are presented in Fig. 5. Data from column strain and bars strain was recorded using electronic data-logger attached to the computer. In addition, load was recorded automatically using a 5000 kN dynamometer to determine the Load-strain diagram of specimens. Precision and care was taken to ensure that the columns were located in the center of the jack when placed in the machine. Fig. 6 presents test setup and placement of specimens.


Fig. 5 Axial and lateral strain-gage installation place

## 5. Analysis of test results

### *5.1 Ultimate capacity of columns*

The ultimate strains and capacity of columns are presented in Table 5. Table 5 and Fig. 7 show that using single and double layer CFRP in columns without GRP


Fig. 6 Test setup and columns placement in jacks

Table 5 Ultimate strains and capacity of columns

| Column name | Ultimate capacity (kN) | Mean axial strains ($10^{-6}$ mm/mm) | Lateral strain ($10^{-6}$ mm/mm) |
|---|---|---|---|
| N | 566 | * -3848 | 1356 |
| NF1 | 715 | -4144 | 1579 |
| NF2 | 763 | -5432 | 2022 |
| GN | 2485 | -15229 | 4051 |
| GNF1 | 2765 | -18738 | 5347 |
| GNF2 | 2940 | -22075 | 5993 |
| H | 727 | -3848 | 1745 |
| HF1 | 815 | -4451 | 1861 |
| HF2 | 1014 | -5196 | 2304 |
| GH | 2672 | -16429 | 4642 |
| GHF1 | 2897 | -19622 | 5419 |
| GHF2 | 3076 | -23029 | 6336 |

* The negative sign means strain is negative (length reduces)

casing ultimately increased capacity by 26% and 35% for NC columns and 12% and 39% for HSC columns. In addition, with the use of single and double layer CFRP in columns with GRP casing, ultimate capacity increased by 11% and 18% for NC columns and 8% and 15% for HSC columns. As seen using CFRP wrapping for columns without GRP casing increased the ultimate compressive load significantly, while their effect was little in case of the columns with GRP casing due to the effect of GRP confinement.

As depicted Fig. 8, using GRP casing increased the load capacity significantly, RCC capacity increased by 3 times in the NC group and 2.38 times in HSC group averagely.

Using single and double CFRP wrapping layers increased the ultimate axial strain of NC columns by 17% and 43%, respectively, while these values are 15% and 38% in HSC group. Also using GRP casing increased the

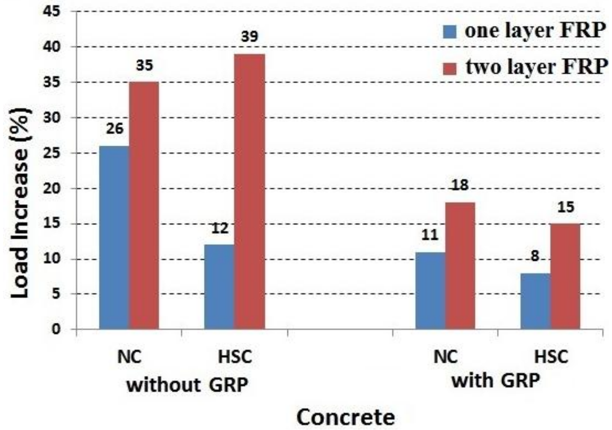


Fig. 7 CFRP effect on compressive capacity of columns

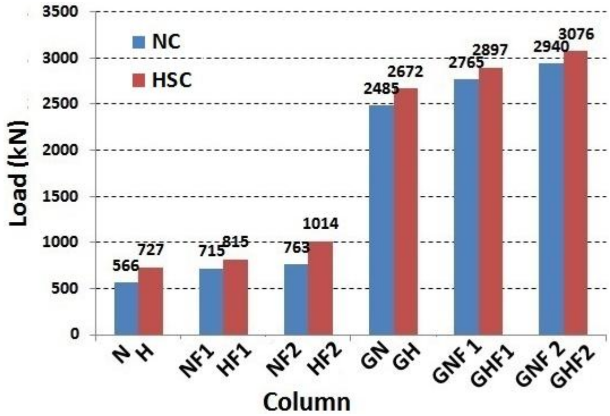


Fig. 8 Compressive capacity of columns

ultimate axial strain of the RCC by mean 295% and 269% in the NC group and HSC group, respectively. The high efficiency of GRP casings on axial strain can be attributed to the presence of fiber in their structure. Therefore, using GRP casings in regions requiring ductile design can be very useful.

### *5.2 Load-strain diagram for columns*

For comparing columns behavior, the load-strain diagrams for axial and lateral strains are presented in Fig. 9.

It is seen from the load-strain diagram that wrapping the RCC with CFRP material increased their radial and axial strains. Furthermore, there was significant increase in the load capacity in these columns.

More precise study of load-strain diagram of columns without GRP casing showed that this curve is made of two parts, linear and non-linear softening parts; change in column behavior is sudden and exhibits pressure crack in concrete, with the commencement of the use of CFRP wrapping, and this strength was maintained under the pressure loads. In addition, load-strain diagram of columns with GRP casing also are made of two parts, linear hardening and non-linear softening, but a change in column behavior is gradual because of the complete integration and more confinement of GRP casing with concrete column. Moreover, it was observed that wrapping columns with

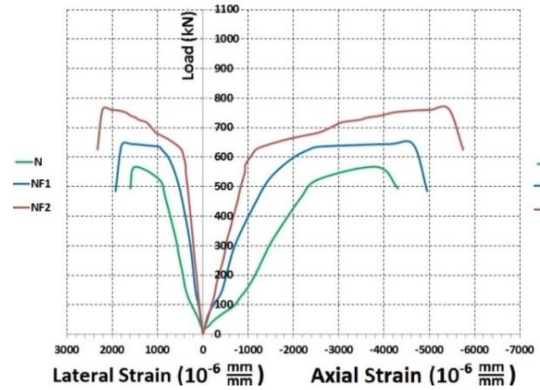


(a) NC group without GRP casing

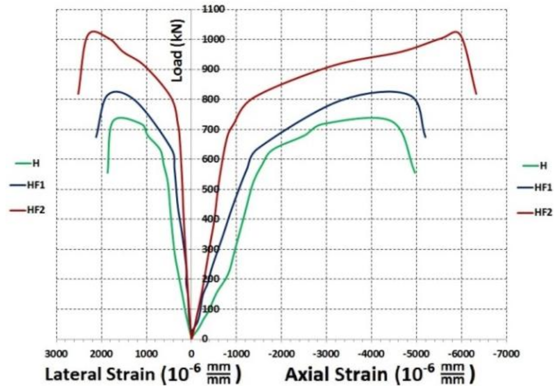


(b) HSC group without GRP casing

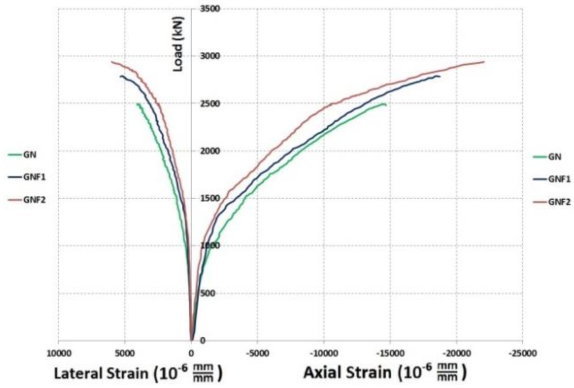


(c) NC group with GRP casing

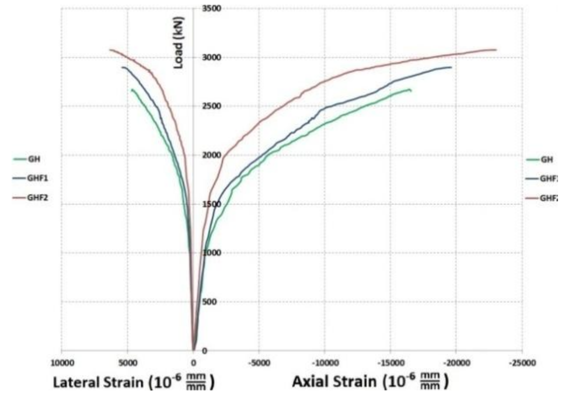


(d) HSC group with GRP casing

Fig. 9 Load-strain diagram for columns with GRP casing

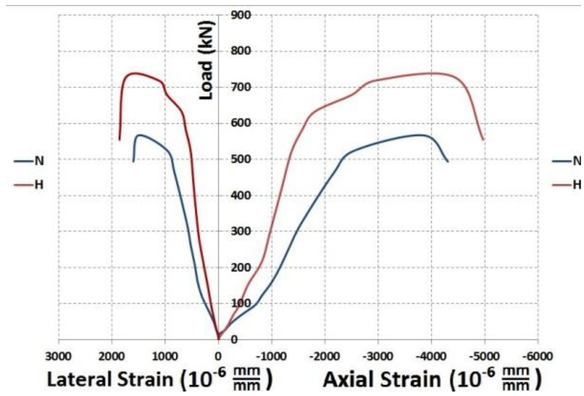


(a) N and H columns

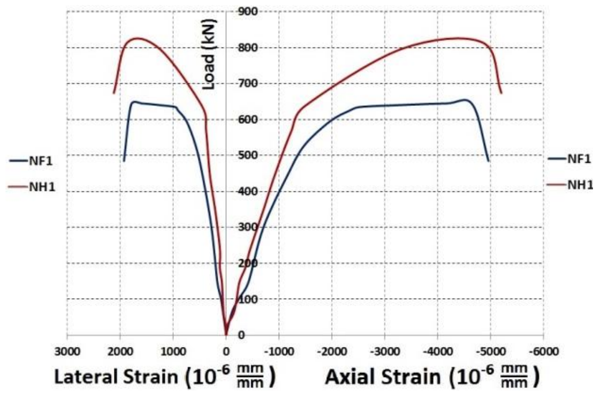


(b) NF1 and HF1 columns

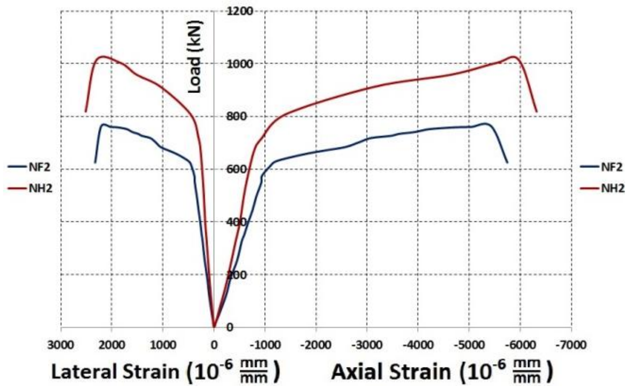


(c) NF2 and HF2 columns

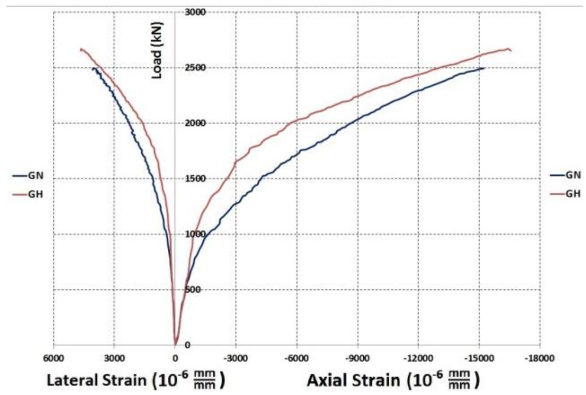


(d) GN and GH columns

Fig. 10 Load-strain diagram for columns with NC and HSC

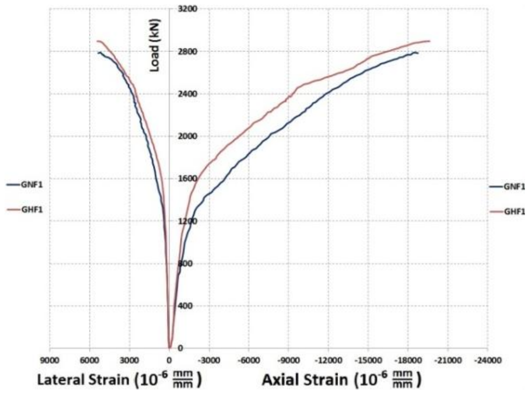


(e) GNF1 and GHF1 columns

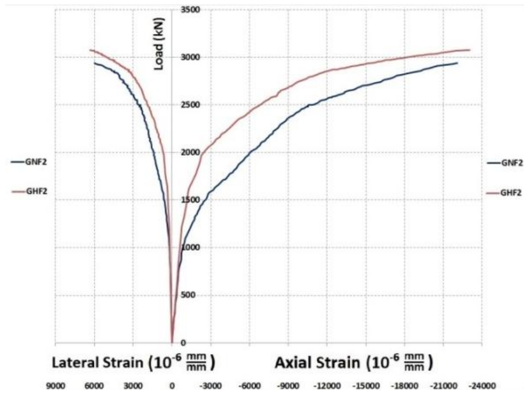


(f) GNF1 and GHF1 columns

Fig. 10 Continued

CFRP increased column stiffness.

For comparing columns behavior with different concrete, the load-strain diagrams for axial and lateral strains are presented in Fig. 10. It is seen from these diagrams that HSC columns have higher compressive capacity and this effect is more in columns without GRP casing, the reason maybe reduction concrete compressive strength effect in compressive capacity of column with GRP casing because the high confinement effect of these casings. Also is seen using HSC increases the axial and lateral strain.

### *5.3 Study of the ruptures of columns*

Columns' rupture is presented in Fig. 11. As can be seen, the rupture of columns in the NC and HSC groups was

N NF1 NF2 GN GNF1 GNF2

(a) NC group

H HF1 HF2 GH GH1 GH2

(b) HSC group

Fig. 11 The rupture of columns after loading similar, most columns' rupture happens due to bars buckling. In columns without GRP casing, the rupture was local and gradual. In these columns, the rupture occurred at one of the two ends due to the fact that the concrete core was less confined by the rebar network at the ends. In columns N and H, which were without CFRP, the compressive cracks formed in the upper part of the columns and pieces were separated from the concrete, the separation of pieces and rebar buckling led to the columns rupture. The columns NF1 and HF1 contained one layer of CFRP and ruptured due to concrete crushing and CFRP tearing on the upper section of the columns; in these columns, unlike the former ones, CFRP wrapping decreased concrete crushing and rebar buckling; therefore, the loading capacities were higher. Columns NF2 and HF2 ruptured similar to NF1 and HF1 with the only difference that the columns rupture and CFRP tearing occurred in the lower section of the columns. In columns without GRP casing, ruptures were gradual and ductile. In columns with GRP casing, rupture modes were different from the columns without GRP casing. In column GN, rupture was complete and occurred in the form of destruction with an explosion sound in the upper section of the column. This type of rupture was due to a very high confinement caused by the GRP casing, which allowed all points of the column to reach their maximum tolerable strain. In addition, it led to the buckling of the longitudinal bars and eventually the rupture of the column. In column GH, the rupture occurred due to the spiral cutting in the middle of the column, and with buckling of the longitudinal bars GRP casing ruptured locally. The rupture of the columns GNF1 and GHF1 were similar to GN with the only difference that more confinement due to the CFRP layer helped the column to stand in a higher strain and eventually rupture in the middle due to buckling longitudinal bars. In columns GNF2 and GHF2, ruptures were similar to the former columns with the difference that more confinement due to the two layers of CFRP led to an overall ruptures in the whole columns after buckling longitudinal bars.

## 6. Numerical modeling of the investigated columns

### *6.1 Columns modeling*

#### *6.1.1 Modeling of material*

The column modeling was done using ABAQUS finite element software. The concrete was modeled using 3D solid elements with 8 nodes (C3D8R), longitudinal and transverse bars were modeled using 3D beam elements (B31), CFRP was modeled using membrane element with 4 nodes (M3D4R), and GRP casing was modeled via 8-node 3D elements (ABAQUS 2011).

In order to determine the non-linear behavior of the concrete, a concrete damage plasticity (CDP) model was used. It is one of the most complicated and practical behavioral models. In order to determine the uniaxial behavior in the curve of the unconfined concrete, the Kent-Park behavioral model was used (Kent and Park 1971). This model is shown in Eq. (3)

$$\sigma_C = f'_{C0}\left[2\left(\frac{\varepsilon_C}{\varepsilon'_C}\right) - \left(\frac{\varepsilon_C}{\varepsilon'_C}\right)^2\right] \tag{3}$$

In Eq. (3), $\sigma_c$ and $\mathcal{E}_c$ are compression stress and axial strain and $f'_{co}$ and $\mathcal{E}'_c$ are cylinder compressive strength of concrete and the corresponding strain, respectively. Park and Paulay reported $\mathcal{E}'c$ to be 0.002 (Park and Paulay 1975). In this research, this parameter was assumed as 0.002.

#### *6.1.2 Confinement effectiveness for sections confined by spirals*

Mander's model was used to define the compressive behavior of the confined concrete. This model relates the compressive strength of the confined concrete with spiral or circular hoops to the unconfined concrete through a coefficient (Mander *et al*. 1988). This behavioral model is summarized according to Eqs. (4) to (7). In these equations, $f'_{cc}$, $f'_{co}$, $f'_l$, $k_e$, $f_{yh}$, $\rho_{cc}$, $\rho_s$, $A_{sp}$, $s'$, $s$, and $d_C$ represent the confined concrete' compressive strength, cylinder compressive strength of the concrete, lateral pressure from the transverse reinforcement, confinement effectiveness coefficient, yield strength of the transverse reinforcement, the ratio of area of longitudinal reinforcement to area of core of section, ratio of the volume of transverse confining steel to the volume of the confined concrete core, area of transverse reinforcement bar, clear vertical spacing between spiral or hoop bars, center to center spacing or pitch of spiral or circular hoop, and core dimensions of centerlines in perimeter hoop, respectively. The effectively confined core for circular hoop reinforcements is shown in Fig. 12. The arrangement of the longitudinal and transverse bars in the finite element model is presented in Fig. 13.

$$f'_{cc} = f'_{co}\left(-1.25 + 2.254\sqrt{1 + \frac{7.94 f'_l}{f'_{co}}} - 2\frac{f'_l}{f'_{co}}\right) \tag{4}$$

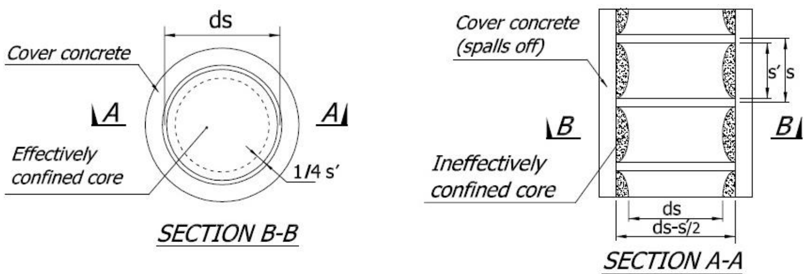


Fig. 12 Effectively confined core for circular hoop reinforcement (Mander *et al*. 1988)

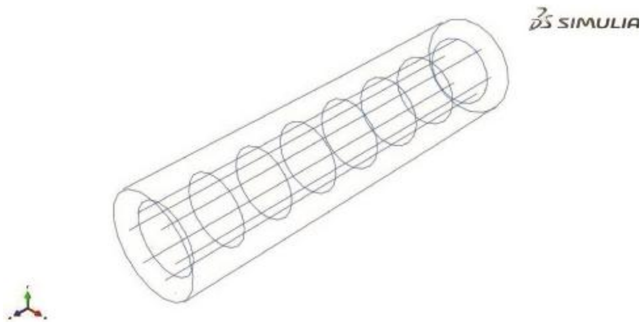

Fig. 13 The arrangement of longitudinal and transverse bars in finite element model

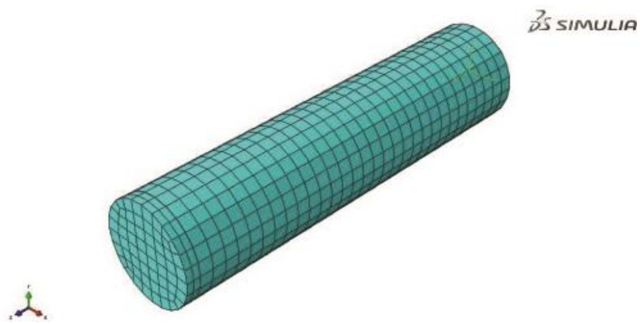

Fig. 14 Meshing method of concrete columns

$$f_l' = \frac{1}{2} k_e \rho_s f_{yh} \tag{5}$$

$$k_e = \frac{1 - \frac{s'}{2d_c}}{1 - \rho_{cc}} \tag{6}$$

$$\rho_s = \frac{4A_{sp}}{sd_s} \tag{7}$$

#### 6.1.3 Modeling of interaction

There are two types of interactions existed in the finite element mesh including the interaction between concrete column and GRP casing and CFRP sheets and the interaction between GRP casing and CFRP sheets that are surface to surface type and the contacts are totally tied. Besides, the interaction between the bars and the surrounding concrete is of an embedded region type (Jiang *et al*. 2014).

The interaction between the concrete and the GRP casing and CFRP sheets and interaction between the GRP casing and the CFRP sheets are modeled by the interface elements available within the ABAQUS element library. The method requires defining two surfaces including the master and slave surfaces. The master surfaces within this model were the GRP and CFRP surfaces surrounding the concrete and the concrete was the slave surface for contacting the concrete to the GRP casing and CFRP sheets. Additionally, the master surface was CFRP surface surrounding the casing and the GRP casing was the slave surface for contacting the GRP casing and CFRP sheets. In addition, the interaction between bars and the surrounding concrete is of the embedded region type, which indicated that the bars were being surrounded by the concrete (Jiang *et al*. 2014).

#### 6.1.4 Boundary conditions, load application, and mesh

In this study, the columns were pinned at both ends. The center of bottom end was restrained to displace in all directions, while the top end was allowed to displace only in the vertical direction. The load was applied as concentrated, axial, and incremental. Moreover, in order to prevent the concentration of stress in the compression area, instead of applying the load to concrete, an element with a high elasticity was defined. Meshing and network diameters were defined to consider accuracy and to help the convergence of responses. The diameter for the elements of the concrete columns, longitudinal and transverse bars, GRP casing, and CFRP sheets were all set to 20 mm (Jiang *et al*. 2014). The meshing of the concrete columns is depicted in Fig. 14.

### 6.2 Numerical analysis results and discussion

#### 6.2.1 load-displacement curve

Axial displacement contour for columns N and H are shown in Fig. 15. As seen in this figure, the maximum axial displacements are occurred at the ends of the columns. Axial load-displacement curve of the studied columns is shown in Fig. 16.

Load-displacement curve shows that by wrapping RCC with CFRP material, load capacity and axial displacement of the columns increased significantly. In Fig. 16, further investigation of load-displacement curves of the columns

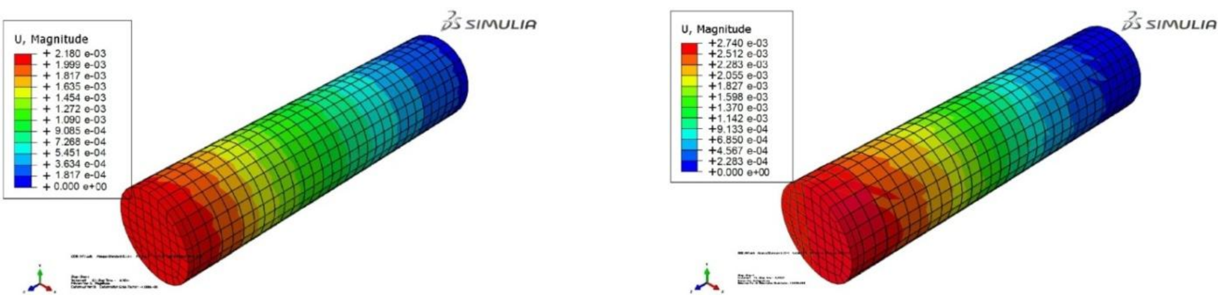


(a) (b)

Fig. 15 Axial displacement contour for (a) column N; (b) column H

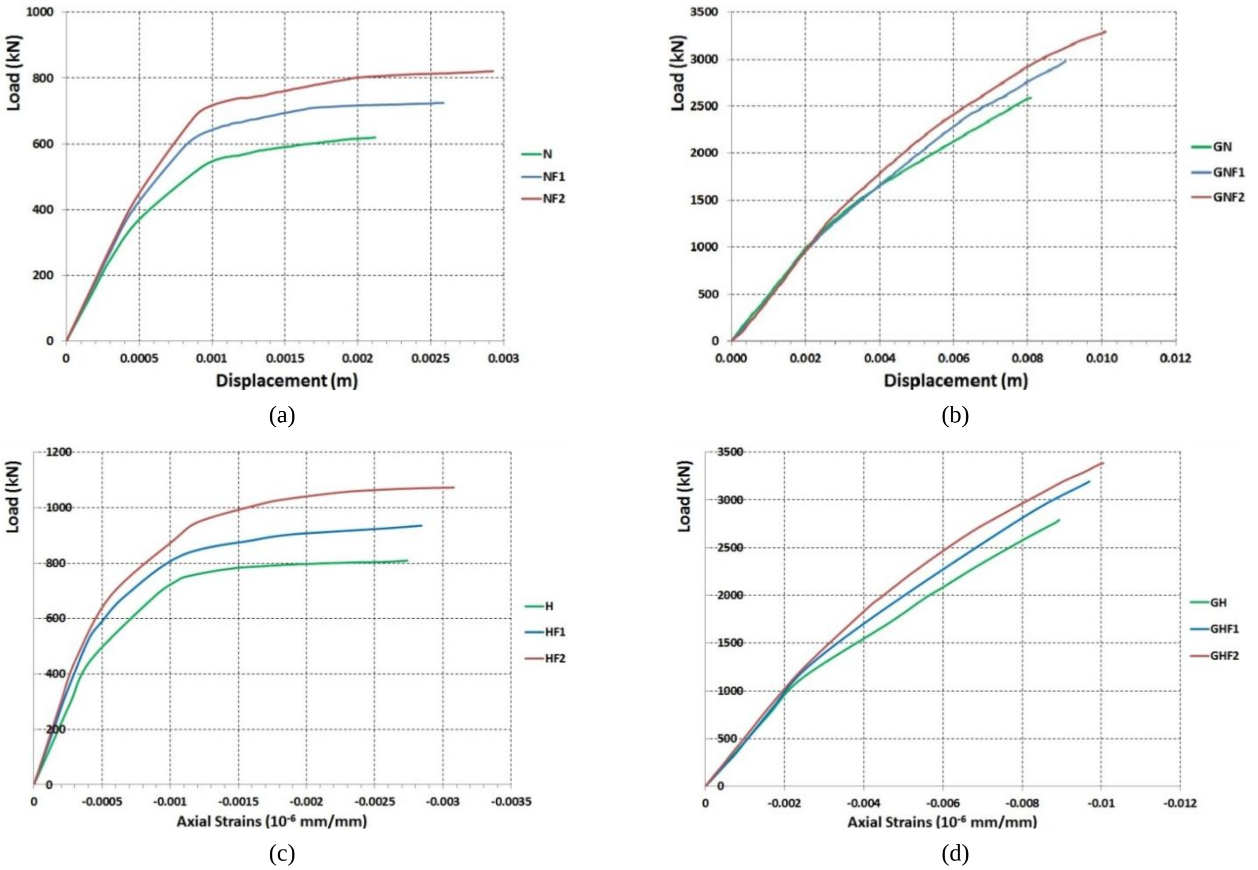


Fig. 16 Axial load-displacement curve for: (a) NC group without GRP casing; (b) HSC group without GRP casing; (c) NC group with GRP casing; (d) HSC group with GRP casing

Table 6 Ultimate load capacity and axial displacement of columns

| Column name | Ultimate capacity (kN) | Axial displacement at maximum load (mm) | The ratio of column ultimate capacity to column N capacity | The ratio of column axial displacement to column N axial displacement |
|---|---|---|---|---|
| N | 619.4 | 2.1 | 1 | 1 |
| NF1 | 724.6 | 2.5 | 1.17 | 1.19 |
| NF2 | 820.8 | 2.9 | 1.32 | 1.38 |
| GN | 2593 | 8.1 | 4.18 | 3.85 |
| GNF1 | 2980 | 9 | 4.81 | 4.28 |
| GNF2 | 3294 | 10.1 | 5.32 | 4.81 |
| H | 809 | 2.7 | 1.31 | 1.29 |
| HF1 | 935.2 | 2.9 | 1.51 | 1.38 |
| HF2 | 1072.7 | 3.1 | 1.73 | 1.48 |
| GH | 2790.8 | 8.9 | 4.51 | 4.23 |
| GHF1 | 3192.9 | 9.8 | 5.15 | 4.67 |
| GHF2 | 3384.8 | 10.5 | 5.46 | 5 |

without casing proves that they consist of linear and non-linear parts. In the linear part, the diagrams have constant slope indicating that until cracks are not formed, columns show the same behavior and while concrete cracks are formed, CFRP wrappings start workings, the behavior of the columns changes and the non-linear part starts. Besides, investigating the load-displacement of the columns with GRP casing in Fig. 16 proves that they also consist of linear and non-linear parts. However, the columns' behavioral change is gradual due to the complete conjunction and more confinement provided by GRP casing.

Table 6 presents the results of compressive ultimate load capacity and axial displacement at maximum load for the columns as well as the effects of the GRP casing and CFRP

Fig. 17 Columns' ductility

| Column name | Columns' ductility (N.m = J) | The ratio of column' ductility to column' N ductility |
|---|---|---|
| N | 990 | 1 |
| NF1 | 1500 | 1.51 |
| NF2 | 1930 | 1.95 |
| GN | 12308 | 12.4 |
| GNF1 | 15453 | 15.6 |
| GNF2 | 18590 | 18.8 |
| H | 1809 | 1.83 |
| HF1 | 2161 | 2.18 |
| HF2 | 2685 | 2.71 |
| GH | 14292 | 14.43 |
| GHF1 | 17824 | 18 |
| GHF2 | 20203 | 20.41 |

sheets on these parameters' changing to column N.

As Table 5 illustrates, using CFRP wrapping to confine columns had a good effect on the column's capacity. In average, using one and two CFRP layers increased columns' ultimate capacity to 15.5% and 29.5%, respectively. Furthermore, using GRP casing was much more effective than CFRP wrapping. In average, GRP casing increased columns' ultimate capacity 2.63 times.

Moreover, in Table 5, ultimate axial displacement comparison shows that using CFRP wrapping has increased this parameter. In average, using one and two layers of CFRP increased axial displacement to 12% and 24%, respectively. Besides, using GRP casing increased the ultimate displacement significantly. In average, using GRP increased displacement 2.5 times.

### *6.2.2 Study of columns' ductility*

In order to compare the ductility of the columns, the area under the load–axial deflection curves (in Fig. 16) was calculated, the results of which are presented in Table 7. The ductility indicates the amount of the energy absorbed by the system or the amount of the work done by an external force on the system.

As depicted Table 6, using CFRP wrapping to confine columns has increased columns ductility. In average, using one and two CFRP layers increased columns' ductility to 30% and 59%, respectively. Next, using GRP casing increased the ultimate displacement significantly. In average, using GRP increased ductility 8.34 times.

## 7. Numerical model verification

In Fig. 17, the load-axial strain curves resulting from the experimental work and the numerical modeling are

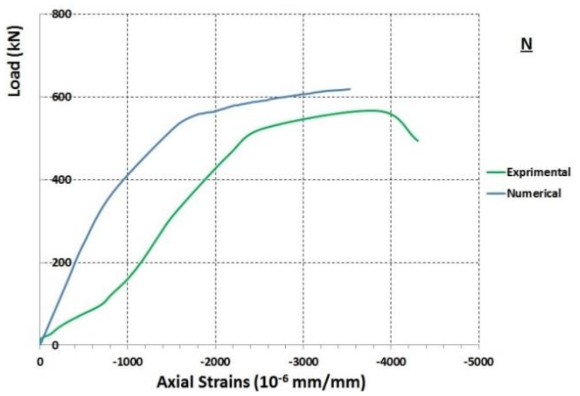


(a)

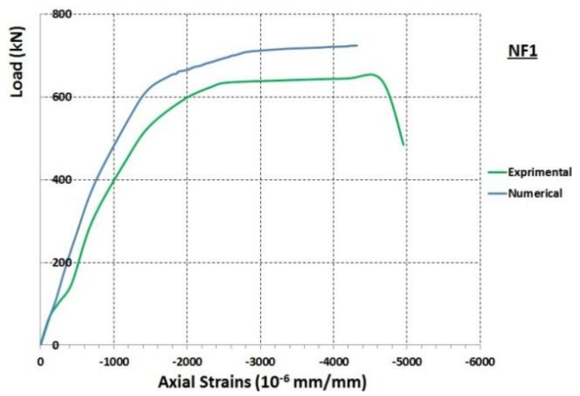


(b)

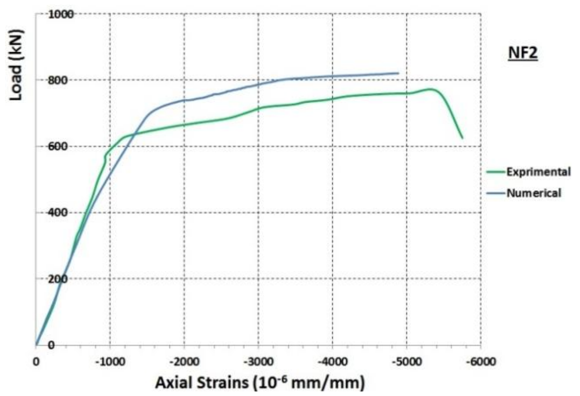


(c)

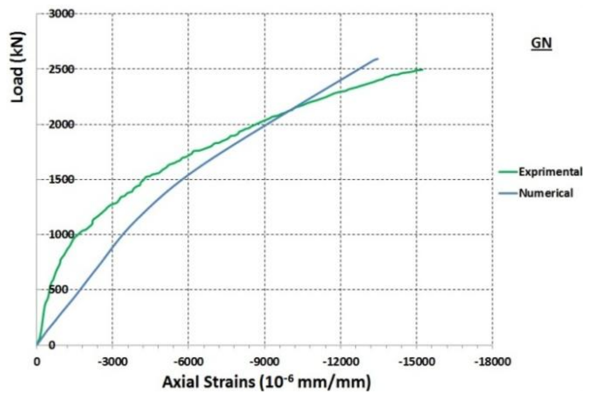


(d)

Fig. 17 Comparison of load-axial strain for experimental work and numerical modeling for: (a) column N; (b) column NF1; (c) column NF2; (d) column GN; (e) column GNF1; (f) column GNF2; (g) column H; (h) column HF1; (i) column HF2; (j) column GH; (k) column GHF1; (l) column GHF2

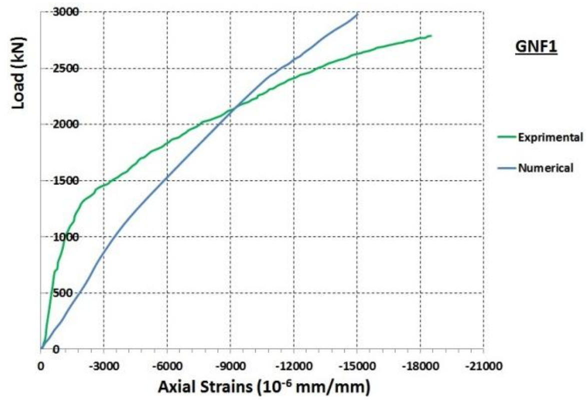


(e)

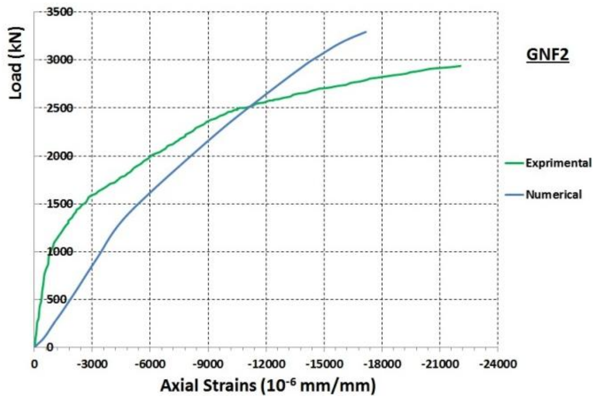


(f)

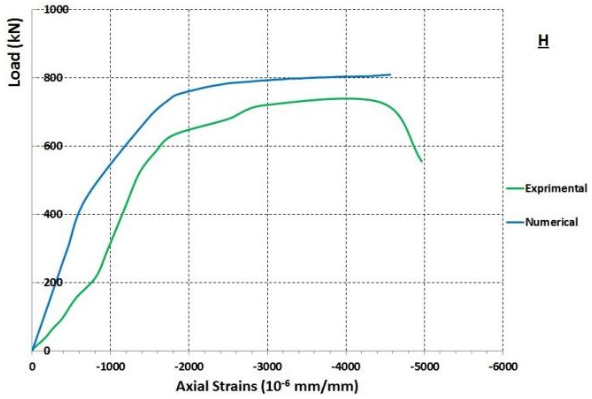


(g)

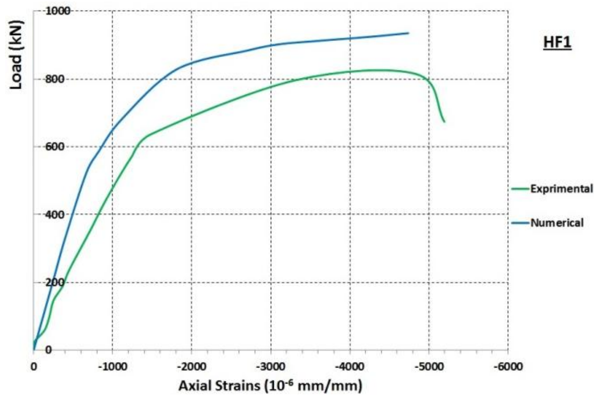


(h)

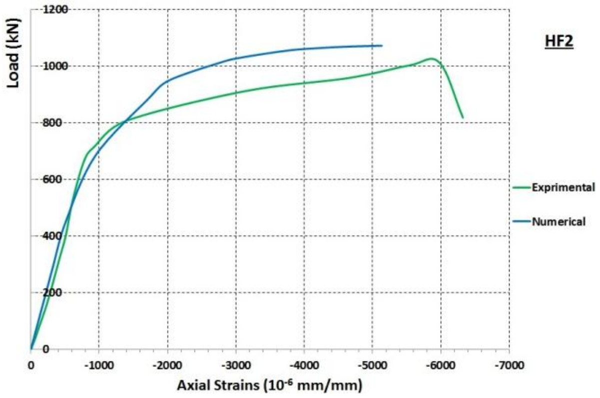


(i)

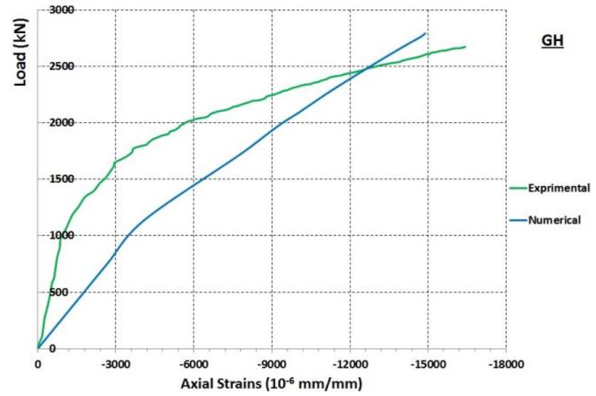


(j)

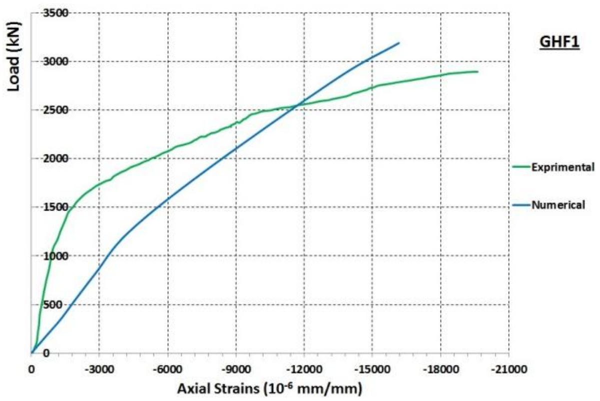


(k)

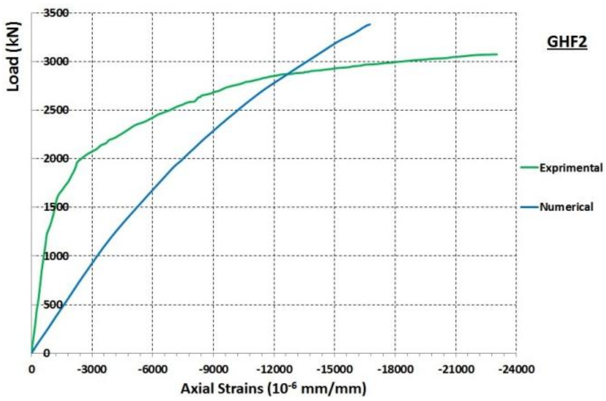


(l)

Fig. 17 Continued

Table 8 Ultimate load capacity and axial strains of experimental work and numerical modeling

| Column name | Ultimate load capacity (kN) | | | Ultimate axial strains ($10^{-6}$ mm/mm) | | |
|---|---|---|---|---|---|---|
| | Experimental work ($P_E$) | Numerical modeling ($P_N$) | $P_N/P_E$ | Experimental work ($S_E$) | Numerical modeling ($S_N$) | $S_N/S_E$ |
| N | 566 | 619.4 | 1.09 | -3848 | -3530 | 0.92 |
| NF1 | 715 | 725.6 | 1.02 | -4650 | -4316 | 0.93 |
| NF2 | 763 | 820.8 | 1.08 | -5432 | -4883 | 0.90 |
| GN | 2485 | 2593 | 1.04 | -15229 | -13460 | 0.88 |
| GNF1 | 2765 | 2980 | 1.08 | -18738 | -15016 | 0.8 |
| GNF2 | 2940 | 3294 | 1.12 | -22075 | -17167 | 0.78 |
| H | 727 | 809 | 1.11 | -4451 | -4575 | 1.03 |
| HF1 | 815 | 935.2 | 1.15 | -5196 | -4738 | 0.91 |
| HF2 | 1014 | 1072.7 | 1.06 | -5976 | -5134 | 0.86 |
| GH | 2672 | 2790.8 | 1.04 | -16429 | -14891 | 0.91 |
| GHF1 | 2897 | 3192.9 | 1.10 | -19622 | -16163 | 0.82 |
| GHF2 | 3076 | 3384.8 | 1.10 | -23029 | -16750 | 0.73 |

presented. Besides, in Table 8, the results of the ultimate loading and strain resulting from the experimental work and numerical modeling are compared. As can be concluded, there is a good convergence between the experimental work and the numerical modeling results.

Despite the good convergence between the results of numerical modeling and the experimental works, the slight difference between the results can be due to the assumptions and simplifications made in modeling and defining the parameters in the logical ranges and according to the model presented in previous studies.

## 8. Conclusions

The overall result of this study is the introduction of a new type of composite columns with reinforced concrete, GRP casing and CFRP sheets. The excellent results of using the GRP casing showed that this casing could be used in constructing new buildings and the CFRP sheets can be used to strengthen concrete columns to increase the load capacity and the ductility of the members.

The key results of this research are as follows:

(1) Using GRP casing as the framework and strengthening of the RCC increased the ultimate compressive load significantly, as the using GRP casing increased the compression capacity of the columns by 3 times in the NC group and 2.38 times in the HSC group.

(2) Strengthening the concrete column via CFRP wrapping in the columns without GRP casing increased the ultimate compressive load significantly, while their effect was little in case of the columns with GRP casing due to the effect of GRP confinement.

(3) The percentage of strengthening generated by CFRP sheets for columns made with NC is higher than that with HSC. The probable reason is the lower strength created by the confining layer relative to the compression strength of the HSC.

(4) Increasing number of CFRP layers increased compressive load capacity of the column, while increasing the load capacity did not have a direct relation with the number of the layers. As the number of layers increased, the increase rate of the load capacity reduced.

(5) Load-displacement curves of the RCC with CFRP and without GRP casing are divided into linear-elastic and softening nonlinear-plastic parts.

(6) Load-displacement curves of the RCC with GRP casing are divided into linear elastic and linear elastoplastic parts. Note that these curves have no descending branches due to the fragility of the GRP casing.

(7) The ultimate displacement of columns with CFRP wrapping was higher than the columns without wrapping. In addition, using GRP casing increased ultimate displacement significantly.

(8) Using CFRP wrapping to strengthen the concrete columns increased their ductility significantly. Besides, the ductility was very great for the columns with GRP casing in comparison with the ones without GRP casing.

(9) CFRP wrapping and the GRP casing effects were greater on enhancing ductility in the NC group.

(10) Investigating columns' failure modes indicated columns without GRP casing ruptured locally and gradually. Furthermore, the columns with GRP casing completely ruptured in the whole column. This type of rupture was due to a very high confinement caused by the GRP casing, which allowed all points of the column to reach their maximum tolerable strain.

## References

ABAQUS, A.S. (2011), User's manual; Version 6.11. 1. Dassaults Systemes Inc.

ACI 211 (1991), Standard practice for selecting proportions for normal, heavyweight and mass concrete.

Abedini, M., Khlaghi, E.A., Mehrmashhadi, J., Mussa, M.H., Ansari, M. and Momeni, T. (2017), "Evaluation of Concrete Structures Reinforced with Fiber Reinforced Polymers Bars: A Review", *J. Asian Sci. Res.*, **7**(5), 165.

Aghaee, K. and Foroughi, M. (2013), "Mechanical properties of lightweight concrete partition with a core of textile waste", *Adv. Civil Eng.*, 1-7.

Almusallam, T.H. (2007), "Behavior of normal and high-strength concrete cylinders confined with E-glass/epoxy composite laminates", *Compos. Part B: Eng.*, **38**(5-6), 629-639.

Andalib, Z., Kafi, M.A., Bazzaz, M. and Momenzadeh, S. (2018), "Numerical evaluation of ductility and energy absorption of steel rings constructed from plates", *Eng. Struct.*, **169**, 94-106.

Ardalan, R.B., Joshaghani, A. and Hooton, R.D. (2017), "Workability retention and compressive strength of self-compacting concrete incorporating pumice powder and silica fume", *Constr. Build. Mater.*, **134**, 116-122.

ASTM, B. (2001), D2996-Standard Specification for Filament-Wound Fiberglass; Glass-Fiber-Reinforced Thermosetting-Resin Pipe.

Bazzaz, M., Darabi, M.K., Little, D.N. and Garg, N. (2018), "A straightforward procedure to characterize nonlinear viscoelastic response of asphalt concrete at high temperatures", *Proceedings of the Transportation Research Record, Transportation Research Board 96th Annual Meeting.* http://journals.sagepub.com/doi/abs/10.1177/0361198118782033

Csuka, B. and Kollár, L.P. (2010), "FRP-confined circular concrete columns subjected to concentric loading", *J. Reinf. Plast. Compos.*, **29**(23), 3504-3520.

Dundar, C., Erturkmen, D. and Tokgoz, S. (2015), "Studies on carbon fiber polymer confined slender plain and steel fiber reinforced concrete columns", *Eng. Struct.*, **102**, 31-39.

Goodarzi, A., Mehrmashhadi, J. and Esmailzadeh, E. (2009), "Optimised braking force distribution strategies for straight and curved braking", *Int. J. Heavy Vehicle Syst.*, **16**(1), 78.

Hamidian, M., Shariati, M., Arabnejad, M. and Sinaei, H. (2011), "Assessment of high strength and light weight aggregate concrete properties using ultrasonic pulse velocity technique", *Int. J. Phys. Sci.*, **6**(22), 5261-5266.

Hamidian, M., Shariati, A., Khanouki, M.M.A., Sinaei, H., Toghroli, A. and Nouri, K. (2012), "Application of Schmidt rebound hammer and ultrasonic pulse velocity techniques for structural health monitoring", *Sci. Res. Essays*, **7**(21), 1997-2001.

Jiang, S.-F., Ma, S.-L. and Wu, Z.-Q. (2014), "Experimental study and theoretical analysis on slender concrete-filled CFRP–PVC tubular columns", *Constr. Build. Mater.*, **53**, 475-487.

Joshaghani, A. (2017), "The effect of trass and fly ash in minimizing alkali-carbonate reaction in concrete", *Constr. Build. Mater.*, **150**, 583-590.

Kazemi, M.T., Momenzadeh, S.-B. and Hoseinzadehasl, M. (2012), "Study of reduced beam section connections with web opening", *Proceedings of the 15th World Conference on Earthquake Engineering*, Lisbon, September.

Kent, D.C. and Park, R. (1971), "Flexural members with confined concrete", *J. Struct. Div*.

Khairallah, F. (2013), "Mechanical behavior of confined self-compacting reinforced concrete circular columns under concentric axial loading", *Ain Shams Eng. J.*, **4**(4), 641-649.

Khanouki, M.M.A., Ramli Sulong, N.H., Shariati, M. and Tahir, M.M. (2016), "Investigation of through beam connection to concrete filled circular steel tube (CFCST) column", *J. Constr. Steel Res.*, **121**, 144-162. DOI: http://dx.doi.org/10.1016/j.jcsr.2016.01.002

Khorami, M., Khorami, M., Motahar, H., Alvansazyazdi, M., Shariati, M., Jalali, A. and Tahir, M. (2017), "Evaluation of the seismic performance of special moment frames using incremental nonlinear dynamic analysis", *Struct. Eng. Mech., Int. J.*, **63**(2), 259-268.

Khorramian, K., Maleki, S., Shariati, M. and Ramli Sulong, N.H. (2015), "Behavior of Tilted Angle Shear Connectors", *PLOS ONE*, **10**(12), 1-11. DOI: 10.1371/journal.pone.0144288

Kumutha, R., Vaidyanathan, R. and Palanichamy, M. (2007), "Behaviour of reinforced concrete rectangular columns strengthened using GFRP", *Cement Concrete Compos.*, **29**(8), 609-615.

Lam, L. and Teng, J. (2003), "Design-oriented stress–strain model for FRP-confined concrete", *Constr. Build. Mater.*, **17**(6-7), 471-489.

Le, H.T.N., Poh, L.H., Wang, S. and Zhang, M.-H. (2017), "Critical parameters for the compressive strength of high-strength concrete", *Cement Concrete Compos.*, **82**, 202-216.

Mander, J.B., Priestley, M.J. and Park, R. (1988), "Theoretical stress-strain model for confined concrete", *J. Struct. Eng.*, **114**(8), 1804-1826.

Mohammadhassani, M., Akib, S., Shariati, M., Suhatril, M. and Arabnejad Khanouki, M.M. (2014a), "An experimental study on the failure modes of high strength concrete beams with particular references to variation of the tensile reinforcement ratio", *Eng. Fail. Anal.*, **41**, 73-80. DOI: http://dx.doi.org/10.1016/j.engfailanal.2013.08.014

Mohammadhassani, M., Nezamabadi-pour, H., Suhatril, M. and Shariati, M. (2014b), "An evolutionary fuzzy modelling approach and comparison of different methods for shear strength prediction of high-strength concrete beams without stirrups", *Smart Struct. Syst., Int. J.*, **14**(5), 785-809.

Mohammadhassani, M., Saleh, A., Suhatril, M. and Safa, M. (2015), "Fuzzy modelling approach for shear strength prediction of RC deep beams", *Smart Struct. Syst., Int. J.*, **16**(3), 497-519.

Momenzadeh, S., Seker, O., Faytarouni, M. and Shen, J. (2017), "Seismic performance of all-steel buckling-controlled braces with various cross-sections", *J. Constr. Steel Res.*, **139**, 44-61.

Paknahad, M., Shariati, M., Sedghi, Y., Bazzaz, M. and Khorami, M. (2018), "Shear capacity equation for channel shear connectors in steel-concrete composite beams", *Steel Compos. Struct., Int. J.*, **28**(4), 483-494.

Park, R. and Paulay, T. (1975), *Reinforced Concrete Structures*, John Wiley & Sons Inc.

Parvin, A. and Jamwal, A.S. (2005), "Effects of wrap thickness and ply configuration on composite-confined concrete cylinders", *Compos. Struct.*, **67**(4), 437-442.

Pessiki, S., Harries, K.A., Kestner, J.T., Sause, R. and Ricles, J.M. (2001), "Axial behavior of reinforced concrete columns confined with FRP jackets", *J. Compos. Constr.*, **5**(4), 237-245.

Plastics, A.C.D.-o. (2010), Standard test method for tensile properties of plastics; ASTM International.

Rahai, A., Sadeghian, P. and Ehsani, M.R. (2008), "Experimental behavior of concrete cylinders confined with CFRP composites", *Proceedings of the 14th World Conference on Earthquake Engineering*.

Saafi, M., Toutanji, H.A. and Li, Z. (1999), "Behavior of concrete columns confined with fiber reinforced polymer tubes" *ACI Mater. J.*, **96**(4), 500-509.

Sadeghipour Chahnasir, E., Zandi, Y., Shariati, M., Dehghani, E., Toghroli, A., Mohamed, E.T., Shariati, A., Safa, M., Wakil, K. and Khorami, M. (2018), "Application of support vector machine with firefly algorithm for investigation of the factors affecting the shear strength of angle shear connectors", *Smart Struct. Syst., Int. J.*, **22**(4), 413-424.

Samaan, M., Mirmiran, A. and Shahawy, M. (1998), "Model of concrete confined by fiber composites", *J. Struct. Eng.*, **124**(9),

1025-1031.
Shahawy, M., Mirmiran, A. and Beitelman, T. (2000), "Tests and modeling of carbon-wrapped concrete columns", *Compos*. *Part B*: *Eng*., **31**(6-7), 471-480.
Sharbatdar, M.K.B., Kashiha, N. and Zahra, A. (2008), "Behavior of Fiber Concrete under Impact and Explosive Load", *Proceedings of the 14th International Civil Engineering Student Conference*, Semnan, Iran.
Shariati, M. (2008), "Assessment Building Using None-destructive Test Techniques (ultra Sonic Pulse Velocity and Schmidt Rebound Hammer)", Universiti Putra Malaysia, Malaysia.
Shariati, A. (2014), "Behaviour of C-shaped Angle Shear Connectors in High Strength Concrete", M.Sc.; Jabatan Kejuruteraan Awam, Fakulti Kejuruteraan, Universiti Malaya, Malaysia.
Shariati, M., Ramli Sulong, N.H., Arabnejad Khanouki, M.M., Shafigh, P. and Sinaei, H. (2011a), "Assessing the strength of reinforced concrete structures through Ultrasonic Pulse Velocity and Schmidt Rebound Hammer tests", *Sci*. *Res*. *Essays*, **6**(1), 213-220.
Shariati, M., Ramli Sulong, N.H., Arabnejad Khanouki, M.M. and Shariati, A. (2011b), "Experimental and numerical investigations of channel shear connectors in high strength concrete", *Proceedings of the 2011 World Congress on Advances in Structural Engineering and Mechanics* (*ASEM*'*11+*), Seoul, South Korea.
Shariati, M., Ramli Sulong, N.H., Sinaei, H., Khanouki, A., Mehdi, M. and Shafigh, P. (2011c), "Behavior of channel shear connectors in normal and light weight aggregate concrete (experimental and analytical study)", *Adv*. *Mater*. *Res*., **168**, 2303-2307.
Shariati, M., Ramli Sulong, N.H. and Arabnejad Khanouki, M.M. (2012), "Experimental assessment of channel shear connectors under monotonic and fully reversed cyclic loading in high strength concrete", *Mater*. *Des*., **34**, 325-331.
DOI: 10.1016/j.matdes.2011.08.008
Shariati, M., Shariati, A., Sulong, N.R., Suhatril, M. and Khanouki, M.A. (2014a), "Fatigue energy dissipation and failure analysis of angle shear connectors embedded in high strength concrete", *Eng*. *Fail*. *Anal*., **41**, 124-134.
Shariati, A., Shariati, M., Ramli Sulong, N.H., Suhatril, M., Arabnejad Khanouki, M.M. and Mahoutian, M. (2014b), "Experimental assessment of angle shear connectors under monotonic and fully reversed cyclic loading in high strength concrete", *Constr*. *Build*. *Mater*., **52**, 276-283.
DOI: http://dx.doi.org/10.1016/j.conbuildmat.2013.11.036
Shariati, M., Ramli Sulong, N.H., Shariati, A. and Khanouki, M.A. (2015), "Behavior of V-shaped angle shear connectors: experimental and parametric study", *Mater*. *Struct*., 1-18.
DOI: 10.1617/s11527-015-0762-8
Shariati, M., Ramli Sulong, N.H., Shariati, A. and Kueh, A.B.H. (2016), "Comparative performance of channel and angle shear connectors in high strength concrete composites: An experimental study", *Constr*. *Build*. *Mater*., **120**, 382-392.
DOI: http://dx.doi.org/10.1016/j.conbuildmat.2016.05.102
Sheikh, S.A. (2002), "Performance of concrete structures retrofitted with fibre reinforced polymers", *Eng*. *Struct*., **24**(7), 869-879.
Sinaei, H., Jumaat, M.Z. and Shariati, M. (2011), "Numerical investigation on exterior reinforced concrete Beam-Column joint strengthened by composite fiber reinforced polymer (CFRP)", *Int*. *J*. *Phys*. *Sci*., **6**(28), 6572-6579.
Testing, A.S.f. and Materials (2004), Standard Test Method for Determining Tensile Properties of Nonreinforced Polyethylene and Nonreinforced Flexible Polypropylene Geomembranes; ASTM International.
Toghroli, A., Darvishmoghaddam, E., Zandi, Y., Parvan, M., Safa, M., Abdullahi, M.A.M., Heydari, A., Wakil, K., Gebreel, S.A. and Khorami, M. (2018a), "Evaluation of the parameters affecting the Schmidt rebound hammer reading using ANFIS method", *Comput*. *Concrete*, *Int*. *J*., **21**(5), 525-530.
Toghroli, A., Shariati, M., Sajedi, F., Ibrahim, Z., Koting, S., Tonnizam Mohamad, E. and Khorami, M. (2018b), "A review on pavement porous concrete using recycled waste materials", *Smart Struct*. *Syst*., *Int*. *J*., **22**(4), 433-440.
Tokgoz, S., Dundar, C. and Tanrikulu, A.K. (2012), "Experimental behaviour of steel fiber high strength reinforced concrete and composite columns", *J*. *Constr*. *Steel Res*., **74**, 98-107.
Vincent, T. and Ozbakkaloglu, T. (2013), "Influence of concrete strength and confinement method on axial compressive behavior of FRP confined high-and ultra high-strength concrete", *Compos*. *Part B*: *Eng*., **50**, 413-428.
Wong, Y., Yu, T., Teng, J. and Dong, S. (2008), "Behavior of FRP-confined concrete in annular section columns", *Compos*. *Part B*: *Eng*., **39**(3), 451-466.
Wu, G., Lü, Z. and Wu, Z. (2006), "Strength and ductility of concrete cylinders confined with FRP composites", *Constr*. *Build*. *Mater*., **20**(3), 134-148.
Xiao, Y. and Wu, H. (2000), "Compressive behavior of concrete confined by carbon fiber composite jackets", *J*. *Mater*. *Civil Eng*., **12**(2), 139-146.
Xiao, J., Tresserras, J. and Tam, V.W. (2014), "GFRP-tube confined RAC under axial and eccentric loading with and without expansive agent", *Constr*. *Build*. *Mater*., **73**, 575-585.
Youssef, M.N., Feng, M.Q. and Mosallam, A.S. (2007), "Stress–strain model for concrete confined by FRP composites", *Compos*. *Part B*: *Eng*., **38**(5-6), 614-628.

*CC*